Simulation of thermal behaviours and powder flow for direct laser metal deposition process

Quanren Zeng[1], *Yankang* Tian[1], *Zhenhai* Xu[1, 2] and *Yi* Qin[1,*]

[1] Department of Design, Manufacture and Engineering Management, University of Strathclyde, G1 1XQ, Glasgow, UK
[2] National Key Laboratory for Precision Hot Processing of Metals & School of Materials Science and Engineering, Harbin Institute of Technology, Harbin 150001, China

Abstract. Laser engineering net-shaping (LENS), based on directed energy deposition (DED), is one of the popular AM technologies for producing fully dense complex metal structural components directly from laser metal deposition without using dies or tooling and hence greatly reduces the lead-time and production cost. However, many factors, such as powder-related and laser-related manufacturing parameters, will affect the final quality of components produced by LENS process, especially the powder flow distribution and thermal history at the substrate. The powder concentration normally determines the density and strength of deposited components; while the thermal behaviours of melt pool mainly determines the cooling rate, residual stress and consequent cracks in deposited components. Trial and errors method is obviously too expensive to afford for diverse applications of different metal materials and various manufacturing input parameters. Numerical simulation of the LENS process will be an effective means to identify reasonable manufacturing parameter sets for producing high quality crack-free components. In this paper, the laser metal powder deposition process of LENS is reported. The gas-powder flow distribution below the deposition nozzle is obtained via CFD simulation. The thermal behaviours of substrate and as-deposited layer/track during the LENS process are investigated by using FEM analysis. Temperature field distributions caused by the moving laser beam and the resultant melt pool on the substrate, are simulated and compared. The research offers a more accurate and practical thermal behaviour model for LENS process, which could be applied to further investigation of the interactions between laser, melt pool and powder particles; it will be particularly useful for manufacturing key components which has more demanding requirement on the components' functional performance.

Keywords: Additive manufacturing, Powder, Simulation

1 Introduction

Laser engineering net-shaping (LENS), based on a kind of directed energy deposition (DED), is one of the popular AM technologies for producing complex metal structural components production. It could be used to fabricate complex, fully-dense metal components from CAD files directly without using dies, tooling or further machining, which hence greatly reduces the lead-time and production cost. Although LENS is a promising additive manufacturing process, it has not been widely used until recently. One of the main reasons is the high temperature and cooling rate during the LENS process will produce large residual stresses which may cause detrimental cracks and geometrical distortion to the deposited components. Besides, the range of deposited component size, imperfect surface quality and high cost of metal powder also limited LENS applications. Many factors, such as the laser-related and powder-related input manufacturing parameters will affect the final quality of components produced by LENS process, especially the thermal history of laser metal-powder deposition process mainly determining the cooling rate, residual stress and consequent cracks on the surface of deposited components. Trial and errors method is obviously too expensive to afford for diverse applications of different metal materials and various manufacturing input parameters. Numerical simulation of the LENS process will be an effective means to identify reasonable manufacturing parameter sets for producing high quality crack-free components.

Many researches have already tried to investigate the LENS or direct laser metal deposition (LMD) process numerically or experimentally [1-4]. Peyre et al [5] developed a three-step analytical and numerical approach to predict the shapes of manufactured structures and thermal loadings induced by the LMD process using multi-physics COMSOL. This approach takes into account the moving interface during metal deposition which allows the conductivity front to move simultaneously with the moving laser source and hence could accurately represent the LMD process. Liu et al. [6] proposed a FE model to predict thermal stress and

* Corresponding author: qin.yi@strath.ac.uk

deformations generated in the multi-layer laser metal deposition process. The thermal distribution, thermal stress field, geometry deformation and effect of deposition parameters on residual stress and deflections are explained. Verma et al [7] managed to simulate the thermal effect of a moving heat source on the SS316 and Ni substrates for LMD using Ansys Parametric Design Language. Manvatkar et al [8] developed a three-dimensional, transient, heat transfer, and fluid flow model for the laser assisted multilayer additive manufacturing process with coaxially fed austenitic stainless steel powder. Johnson et al [9] simulated the thermo-mechanical history and 3D microstructure evolution of 304L stainless steel tubes manufactured using LENS. Stender et al [10] proposed the process modelling of the LENS process in which thermal mechanical finite element simulation was focused.

Although many modelling and experimental researches relating to the LENS/LMD process have been done, less of them considered the metal powder dynamics effect on the final thermal mechanical behaviors during the LENS. In this paper, the laser metal powder deposition process of LENS is reported. The gas-powder flow distribution below the deposition nozzle is obtained via CFD simulation. The thermal behaviours of substrate and as-deposited layer/track during the LENS process are investigated by using FEM analysis. Temperature field distributions caused by the moving laser beam and the resultant melt pool on the substrate, are simulated and compared. The research offers a more accurate and practical thermal behaviour model for LENS process, which could be applied to further investigation the interactions between laser, melt pool and powder particles; it will be particularly useful for manufacturing key components which has more demanding requirement on the components' functional performance.

1.1 Physical phenomena involved in LENS process

For the LENS process, as shown in Fig.1, a high-power laser is used to melt metal powder supplied

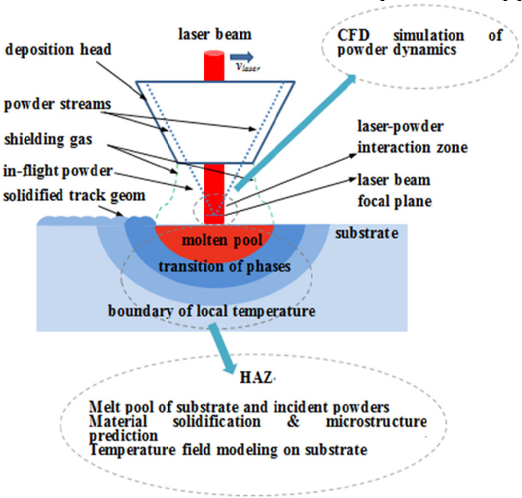

Fig. 1. Schematic diagram of LENS process and involved physical phenomena

coaxially to the focus of the laser beam through a deposition head in LENS. The laser beam typically travels through the centre of the laser deposition head and is focused to a small spot by one or more lenses. The laser head moves horizontally to scan the layer area to be deposited and then will be moved up vertically as each layer is completed. Metal powders are delivered and distributed around the circumference of the head by using a pressurized carrier gas. An inert gas is also used to shield the melt pool from atmospheric oxygen for better control of properties, and to promote layer to layer adhesion by providing better surface.

1.2 Interactions of sub-processes in LENS

To better understand the physic phenomena of LENS process, it is necessary to use a combination of modelling methods to simulate different sub-processes at the corresponding stages in the LENS process first. As seen in Fig.2, there are at least 4 sub-processes to model and simulate for the whole LENS process: (1) powder dynamics; (2) melt pool temperature field formation; (3) solidified track with microstructure evolution; (4) machining (if needed). Linking variables, such as particle mass concentration (PMC), velocity, temperature field of melt pool, cooling rate and residual stress, are transferred in-between different sub-processes for the holistic analysis.

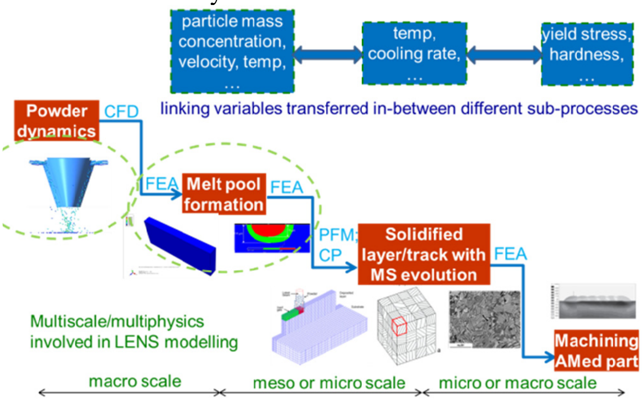

Fig. 2. Numerical realization of whole LENS process by linking different sub-processes

As for the powder dynamics, CFD modelling of the gas-powder flow and powder distribution is key to the density and strength of deposited components. As for the melt pool formation, the moving temperature field on the substrate caused by moving laser heat source is critical to determine the cooling rate, residual stress and consequent cracks in deposited components.

To study the influence of gas-powder flow and thermal behaviour during LENS process on the deposited components and its mechanical properties, accurate modelling, analysis and optimisation of these corresponding sub-processes are indispensable.

2 Modelling gas-powder flow in LENS

Generally, the gas-powder flows in the nozzles' passages and within the interaction zone between the nozzles' tips and the substrate are not a simple one-phase turbulent flow. In fact, this flow can be characterized as a two-phase flow, in which the primary phase is the turbulent inert gas and the secondary phase consists of the metal powder particles. The behavior of particles in a turbulent flow depends on the properties of both the particles and the flow. Turbulent dispersion of both the particles and the carrier gas can be handled by the concept of eddy diffusion energy in some range of the particle size distribution. The interaction of the particle and gas could be solved by two-way coupling the discrete and continuous phase until the solutions in both phases achieve a kind of stable balance. To realize the simulation and analyse powder flow behaviours involved in the powder feeding system of the LENS deposition head, especially the turbulence phenomenon for the gas-powder flow, a CFD numerical model has been developed based on the real nozzle setup shown in Fig.3(a).

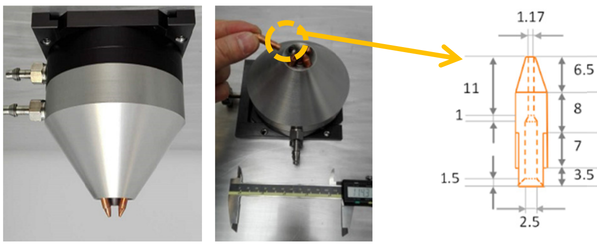

(a) laser deposition head of LENS system (b) size of nozzles

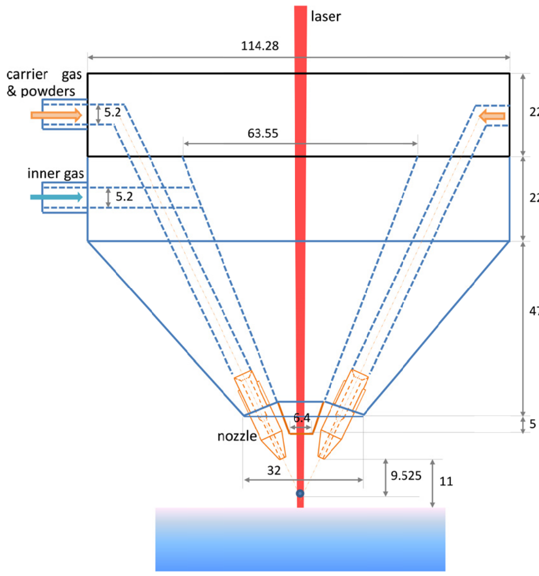

(c) measured geometrical size of LENS laser deposition head

Fig. 3. The laser deposition head with its real geometry of internal passages for CFD simulation

As shown in Fig3(a), the typical construction of a laser deposition head is a conical metal structure with 4 copper powder nozzles facing to a focal point and 1 main central nozzle for gas and laser passing through coaxially. The real geometry of the copper nozzle with internal passages and ducts are given in Fig.3(b). Fig.3(c) shows the schematic diagram of how the laser deposition head deliver powders with assistance of gas and gives detailed geometry with internal passages and ducts are. The gas-powder mixture is firstly injected into the inlets of laser deposition head and reaches a fully developed flow while travelling through the passages and ducts inside the deposition head and nozzles. Once the gas-powder flow is sprayed out from the 4 nozzles' tips, 4 gas-powder mixed jets will firstly flying without interactive actions and then intersect with each other to form a small circular focused spot which show the maximus powder mass concentration of the gas-powder flow.

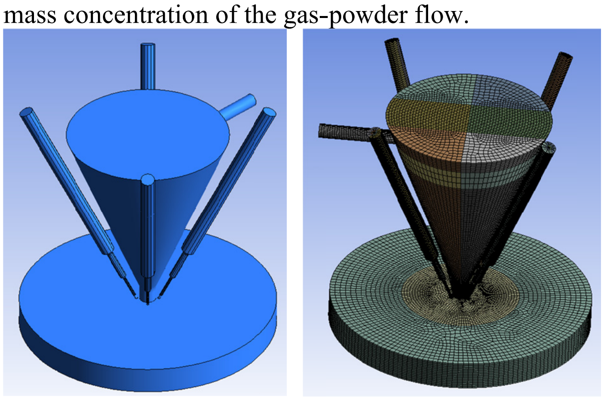

(a) extracted volume for CFD (b) discretized domain for CFD

Fig. 4. Extracted closed volume of LENS deposition head for CFD simulation & its meshes

For CFD simulation, only the closed volume of the laser deposition head is the boundary condition within which the fluid flow will be analysed. Fig. 4(a) shows the extracted geometry for CFD simulation of the powder dynamics. The external area shown in Fig.4(a) is where the powders ejected from the internal nozzle and in-flight until contact with the top surface of the substrate. Fig.4(b) discretizes the CFD domain with different grades of meshes. Near the nozzle's tip, much more refined meshes were used to consider the improvement of overall calculation speed and the required accuracy at some local critical areas with complicated geometry (such as the nozzle tip and focus plane). Some assumptions are taken for modelling of the gas-powder flow: (1) gas-powder mixture is treated as a steady-state turbulent flow with a constant velocity and pressure distribution at the inlets in which k-ε turbulent model is adopted; (2) the powder particles volume fraction is less than 10% and the one-way coupled discrete phase modelling (DPM) is adopted; (3) the heat transfer by laser radiation is temporarily neglected; (4) the particle size is assumed to be spherical and with an average diameter of 100um. For the CFD simulation, a 25L/min argon jet is supplied and ejected from the inner gas nozzle to protect the laser optics from the rebounding particles and to shield the melt pool. The TiAl powders were delivered to the melt pool by using carrier gas (argon) via 4 nozzles which are spaced equally around the inner gas nozzle. The total flow rate of the carrier gas for the 4 nozzles is 5 L/min. These 4 nozzles are installed around the main inner gas nozzle and point to the melt pool which could make the carrier gas-powder jets be trapped to the melt pool. The diameter of the nozzle tip is 1.17mm. Each of the nozzles is titled 65 degree from the substrate surface. The initial conditions for CFD simulation of gas-powder flow are given and listed in Table 1.

Table 1. Input parameters from CFD simulation of gas-powder flow

Inputs for CFD	Value
average diameter of powders	100um
powder flow rate	100g/h
powder flow velocity	0.118 m/s
carrier gas flow rate	8.33×10^{-5} m^3/s
carrier gas flow velocity	0.588 m/s
pressure of carrier gas at inlet	8 bar
pressure of inner gas at inlet	2 bar
inner gas flow rate	6.67×10^{-5} m^3/s
inner gas flow velocity	0.471m/s
nozzle outer diameter	22.56mm
material density	3910kg/m^3
carrier gas density	1.67 kg/m^3
stand-off	9.525mm

3 Thermal behaviour modelling in LENS

3.1. Laser heat source caused temperature field on the substrate

A 3D FE model for simulation of the thermal transfer when laser heat source moving on the substrate is established with user subroutine DFlux in ABAQUS. The transient heat conduction equation between the moving laser heat source and the substrate could be expressed as follow in the 3D Cartesian coordinate system :

$$\frac{\partial}{\partial x}\left(k\frac{\partial T}{\partial x}\right)+\frac{\partial}{\partial y}\left(k\frac{\partial T}{\partial y}\right)+\frac{\partial}{\partial z}\left(k\frac{\partial T}{\partial z}\right)=\rho_s C_s\frac{\partial T}{\partial t} \quad (1)$$

where, k is the thermal conductivity; ρ_s is the substrate material density; C_s is the specific heat; T is the temperature and t is time variables. The typical boundary conditions are represented as

$$q_s = \underbrace{k_n\frac{\partial T}{\partial n}}_{\text{Conduction}} + \underbrace{h_c(T-T_R)}_{\text{Convection}} + \underbrace{\sigma_{S-B}\varepsilon_c(T^4-T_R^4)}_{\text{Radiation}} \quad (2)$$

where n refers to the direction vertical to the substrate surface; k_n is the thermal conductivity vertical to the substrate surface; h_c is the surface heat transfer coefficient; ε_c is emissivity constant; $\sigma_{S\text{-}B}$ is Stefan–Boltzmann constant; T_R is the reference temperature, respectively. The 1st term on the right-hand side in Eq. [4] represents heat energy being transferred to the substrate due to thermal conduction from the surface whose unit normal is n. The 2nd and the 3rd terms on the right-hand side refer to convection and radiation from the surface open to air. For laser beam heat source which follows Gaussian distribution, the heat flux, q_s, transferring from laser beam to the substrate surface could be expressed as:

$$q_s = \frac{\eta P d}{\pi \cdot r_{lb}^2}\exp\left(-\frac{d(x^2+y^2)}{r_{lb}^2}\right) \quad (3)$$

where P is the laser power; η is the thermal absorption coefficient of the laser beam, r_{lb} the radius of the laser beam spot; d is the beam distribution parameter, respectively. The values of d, r_{lb}, and η are considered as 3.0, 0.26 mm, and 0.28, respectively. It is worthy to mention that the high value of d(>2.0) allows the distribution of the applied heat flux to follow a high peak with a steep descent within a small focused area, which is typical for the type of laser used in the LENS machine.

The effective beam radius r_{lb} could be obtained by measuring several melt pool radii that are produced by the LENS system's laser on a SS316 substrate without any powder material. The absorption coefficient, η, of the laser beam is a complex function of substrate temperature, incident surface quality, and shielding atmosphere. To avoid complexity, an average value of η is estimated following Bramson's equation as [3,11]

$$\eta = 0.365\left(\frac{R}{\lambda}\right)^{1/2} - 0.067\left(\frac{R}{\lambda}\right) + 0.006\left(\frac{R}{\lambda}\right)^{3/2} \quad (4)$$

where R is the temperature-dependent electrical resistivity of the material and λ is the wavelength of the laser beam, the latter being equal to 1.067um in the present case.

During the LENS processing, the powders travel through the passages within the laser deposition head and are then ejected out from the nozzles; they will fly to the focus of the laser beam and finally fall into the melt pool if not fully being melt when flying via the focus of laser beam. It is too complicate to track the real-time position and temperature of the individual powders. It is a reasonable assumption that most of the incident powders will be trapped by the molten pool at melting points and some of them may be renounced by the substrate due to large momentum and keeps the room temperature.

In this paper, three-dimensional 8-node heat transfer brick element (DC3D8 in ABAQUS) with temperature as the nodal degree of freedom is used for modelling the moving laser caused thermal behaviours on the substrate. The transient heat transfer calculations are performed using a uniform time-step and a number of very small time increments within each time-step. For the moving laser beam of a moving speed 5m/s and spot diameter of 0.26mm, the simulated temperature field around the laser spot on the substrate are obtained in Section 4. The realization and the application of the heat input to the heat transfer elements in the substrate are realized through an ABAQUS user subroutine DFlux.

4 Simulation & Results

4.1 Gas-powder flow

As mentioned in Fig.2, there are many output variables from CFD simulation, such as particle velocity, particle mass concentration (PMC), DPM number of collision and trajectory of powders after being ejected from the nozzles. PMC is the most important variable

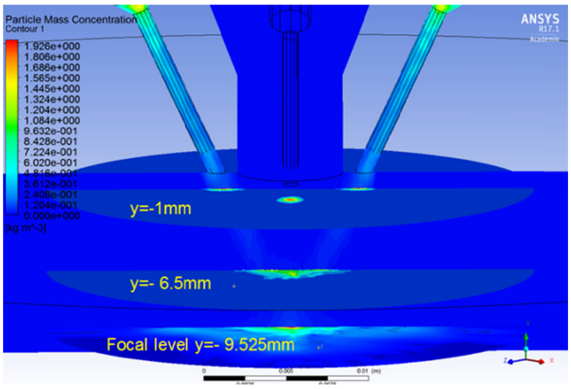

(a) PMC at different distances

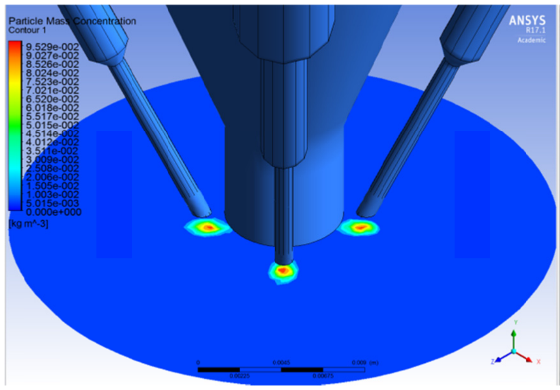

(b) PMC at the level y=-1mm

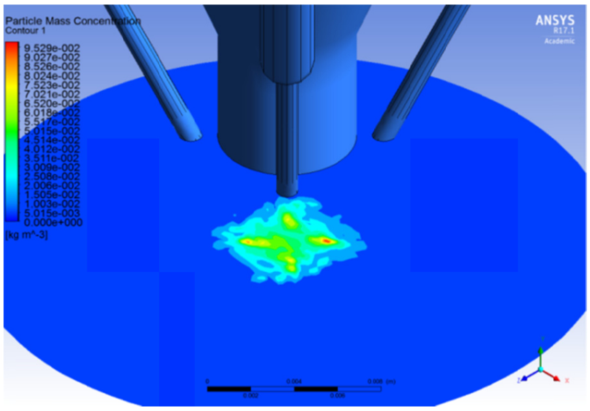

(c) PMC at the level y=-6.5mm

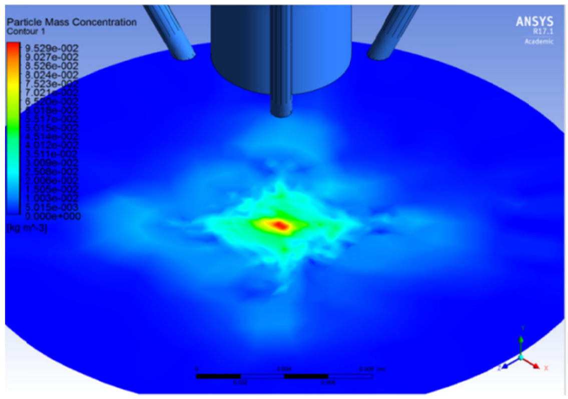

(d)PMC at the focus y=-9.525mm

Fig. 5. PMC at different locations away from the tips of nozzle

determining the density of particles on a specified plane or in a specified volume. It could give the straightforward impression where the particles are more likely to gather.

Fig.5(a) shows the simulated result of variation of particle mass concentration along the stand-off distance of LENS. After ejecting out from the nozzles, there is a clear trend that the 4 jets of particles are travelling to and concentrating on a point of intersection. At the level of y=-1mm (Fig.5(b)), the particle mass concentration of the 4 jets are separate and discrete. When the jets travels to the level of y=-6.5mm (Fig.5(c)), the boundary of 4 jets is becoming blurred. When the 4 jets travels to the level of y=-9.525mm (Fig.5(d)), the highest particle mass concentration of the 4 jets seem to converge at the middle of the domain. If the focal point of a laser beam is just at this location, then the highest laser power heat could be employed to melt the densest cloud of particles. Matching the laser beam focal point and the position of the convergent highest particle mass concentration is extremely important for full fusion of the deposited substrate and particles and consequently generation of crack-free and high-quality deposited tracks. The Fig.5(d) shows a larger influencing area of particle mass concentration than that of Fig.5(b) and (c). It is mainly because that it is near the focal point and some particles will collide and even bounce back once comes into contact with the substrate.

4.2 Thermal behaviors

The laser-related processing parameters and substrate geometry are influential factors for the quality of component produced by LENS process. For the thermal behaviour modelling and simulation, the substrate material is stainless steel (SS316) and its geometry is simplified to be a rectangular block with a size dimension 150mm×60mm×15mm. The bottom and the left side of the workpiece are applied with fixed boundary condition. Substrate material SS316L is assumed to be isotropic and follows Johnson-cook plastic criterion. No material phase transformation is considered. The laser power is 1000W, laser moving velocity 50mm/s. DFlux subroutine is used for simulating the temperature field on the substrate caused by the moving laser beam heat source and the heat flux coming from a laser beam is assumed to follow Gaussian distribution

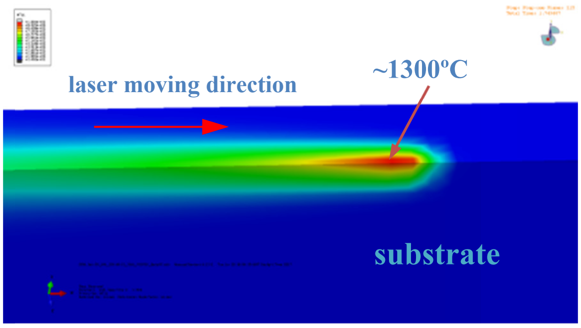

Fig. 6. Moving temperature distribution on the substrate after the LENS process achieving quasi-stable state (t=0.89s)

As shown in Fig.6, a transient temperature field caused by the input moving laser beam is obtained via simulation. The temperature field has a steep gradient distribution at the side of laser moving ahead and a comparatively gradual distribution at the side after laser moving. For the situation, the maximum temperature near the laser spot is around 1300 ºC. If the material's melting point is reached, then the area will be the location of melt pool.

5 Conclusions

The laser metal powder deposition process of LENS is investigated and analysed. Numerical simulations of the key sub-processes within the LENS process are carried out. The gas-powder flow distribution below the deposition nozzle is obtained via CFD simulation. The thermal behaviours of substrate during the LENS process are investigated by using FEM analysis. Temperature field distributions caused by the moving laser beam and the resultant melt pool on the substrate are obtained. This research could offer a more accurate and practical thermal behaviour model for LENS process, which could be applied to further investigation the interactions between laser, melt pool and powder particles; it will be particularly useful for manufacturing key components with LENS process which has more demanding requirement on the components' functional performance.

Acknowledgement

The authors would like to acknowledge the support from EU H2020 project MMTECH (GA 633776) for the research reported in this paper.

References

1. H. Qi, J. Mazumder, H. Ki, J. App. Phys. **100**, 024903 (2006); doi: 10.1063/1.2209807
2. F. Bruckner, D. Lepski, E. Beyer, J. Therm Spray Tech., **16**, (2008). DOI: 10.1007/s11666-007-9026-7
3. V.D. Manvatkar, A.A. Gokhale, G. Jagan Reddy, A. Venkataramana, A. De, Metallur. & Mater. Trans. A, **42A** (2011).
4. L.E. Murr, et al., J. Mater. Sci. Technol., **28** (2012).
5. P. Peyre, P. Aubry, R. Fabbro, R. Neveu, and A Longuet, J. Phys. D. Appl. Phys., **41** (2008).
6. H. Liu, T.E. Sparks, F.W. Liou, and D. M. Dietrich, *Proceedings of 24th Solid Freeform Fabrication Symposium*, Austin, TX, August 12-14, (2013)
7. V. Verma, M. Shukla, *Proceedings of the 15th International RAPDASA conference*, Stellenbosch, South Africa, (2014).
8. V. Manvatkar, A. De, T. DebRoy, *Journal of Applied Physics* **116**, *124905* (2014) (https://doi.org/10.1063/1.4896751)
9. K.L. Johnson, T.M. Rodgers, O.D. Underwood, J.D. Madison, K.R. Ford, S.R. Whetten, D.J. Dagel, J.E. Bishoo, Computational Mechanics, Published online Dec (2017) (https://doi.org/10.1007/s00466-017-1516-y)
10. M.E. Stender, L.L. Beghini, M.G. Veilleux, S.R, Subia, J,D. Sugar, *Proceeding of the ASME 2017 Presure Vessels and Piping Conference (PVP2017-65992)*, Waikoloa, Hawaii, USA (2017)
11. V.D. Manvatkar, A. De, A.A. Gokhale, G. Jagan Reddy, *Proceeding of the Materials Science and Technology (MS&T 2011)*, Columbus, Ohio, USA (2011).